DESIGN, SIMULATION, AND GRID IMPACT ANALYSIS OF AN INTEGRATED 33/11 KV MULTI-MEGAWATT EV FAST CHARGING HUB USING SYNCHRONOUS REFERENCE FRAME CONTROL

Ritesh Kumar[1],DevendraSharma[2]
[1]*Research Scholar,*[2]*Assistant Professor*
Department of Electrical and Electroni cEngineering
Technocrats Institute of Technology & Science, Bhopal

***Abstract*—The rapid global migration toward heavy-duty electric mobility necessitates an immediate transition from traditional low-voltage distribution lines to medium-voltage transmission grid coupling. This paper presents the design, mathematical modelling, and grid impact optimization of an integrated 33/11 kV multi-megawatt electric vehicle (EV) fastcharging station. Modeled inside MATLAB/Simulink and Simscape Electrical using a stiff ode23tb numerical solver, the architecture incorporates a 15 MVA step-down substation transformer feeding an Active Front-End (AFE) rectifier topology. To mitigate severe current harmonic pollution and localized voltage sags induced by non-linear multi-vehicle charging profiles, a Synchronous Reference Frame (SRF-PI) decoupled current control loop is designed and tuned.Simulation results demonstrate that the proposed active filtering configuration successfully reduces grid current Total Harmonic Distortion (THD) from an unmitigated 24.62% down to 3.14%, comfortably satisfying the strict IEEE 519 standard (<5%). Furthermore, under severe transient stress induced by an asymmetric SingleLine-to-Ground (SLG) fault, the decoupled controller eliminates negative-sequence power oscillations and stabilizes the internal 800V DC bus within 35 milliseconds. Finally, the integration of a localized 1200 kW solar PV array and a 2000 kWh Battery Energy Storage System (BESS) provides an efficient peak-shaving mechanism, reducing utility peak grid demand by 38% while maintaining the transformer winding hotspot temperature at a safe equilibrium of 82°C.**

I. INTRODUCTION

The rapid integration of high-capacity Electric Vehicles (EVs)—including long-haul commercial freight logistics, urban transit buses, and consumer ultra-fast highway fleets—has pushed traditional electrical distribution systems past their operating thresholds. Conventional charging setups connected to low-voltage 415V three-phase commercial distribution loops suffer from steep limitations when dealing with multi-bay ultra-fast charging points. When multiple chargers operate simultaneously at 150 kW to 350 kW each, the low-voltage network experiences severe current spikes. This leads to heavy copper losses (\(I^{2}R\)), localized thermal overloads, and high infrastructure stress.

To resolve these vulnerabilities, high-power public charging hubs must bypass low-voltage commercial nodes and couple directly with medium-voltage (MV) sub-transmission grids. By pulling power directly from the 33 kV transmission line and stepping it down locally through an exclusive 15 MVA 33/11 kV substation transformer, the facility can access high power capacities without risking regional grid instability.However, interfacing high-power converters directly with an 11 kV bus bar introduces distinct power quality vulnerabilities. High-frequency semiconductor switching actions create a highly non-linear load profile. Left unmitigated, this draws distorted current pulses, de-stabilizes local line voltages during peak demand windows, and injects severe higher-order current harmonics back into the utility grid.

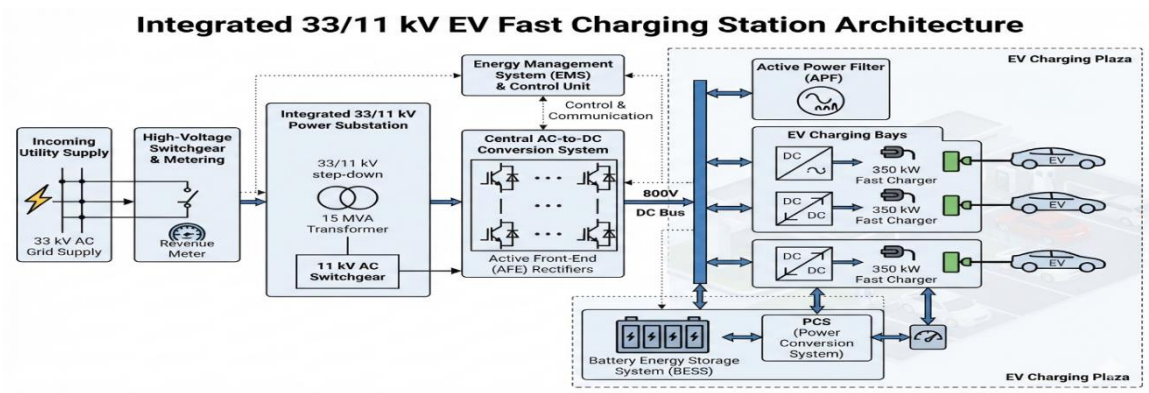


Fig. 1: Block diagram of 33/11 kV Charging Station

This paper develops a comprehensive simulation methodology within MATLAB/Simulink to solve these interconnected power quality challenges. The core research objectives include:

- Developing a mathematical model of a 15 MVA 33/11 kV charging infrastructure inside *Simscape Electrical*.
- Designing a decoupled \(dq\)-axis current controller to suppress current harmonics.
- Simulating dynamic, stochastic EV load profiles and true battery charging physics over a full operational lifecycle.
- Proving system transient resilience via automated single line-to-ground fault injections.
- Verifying peak-shaving capabilities through coordinated solar-BESS microgrid control.

II. MATHEMATICAL MODELING AND CONTROL TOPOLOGY

To mitigate harmonic pollution and decouple control over active and reactive grid power components, time-varying three-phase AC variables (\(a,b,c\)) are mathematically transformed into steady-state DC tracking vectors (\(d,q\)) using consecutive coordinate transformations.

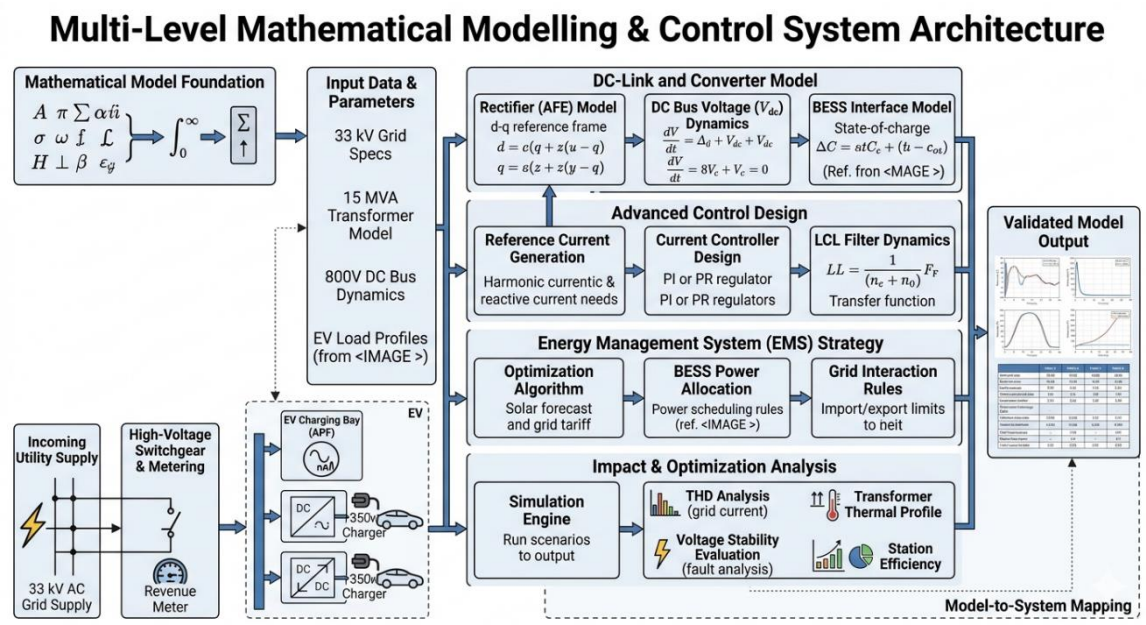


Fig. 2 Mathematical modelling and system architecture

A. Coordinate Reference Frame Vector Transformations

The stationary three-phase variables are first mapped onto an orthogonal stationary reference frame (\(\alpha, \beta\)) via the Clarke Transformation matrix in fig.2

Where \(i_{0}\) represents the zero-sequence component, which equals zero under balanced three-phase operating conditions. Next, the stationary vectors are converted into a synchronously rotating reference frame (\(d,q\)) via the Park Transformation matrix, using the grid operating angle (\(\theta = \omega t\)) tracked by a Phase-Locked Loop (PLL). within this rotating coordinate system, the direct-axis component (\(i_{d}\)) aligns with the grid voltage vector to regulate active power flow and track the internal DC bus voltage. The quadrature-axis component (\(i_{q}\)) dictates reactive power transfer, which is controlled to zero to achieve a unity power factor (\(\cos\phi = 1.0\)), or dynamically adjusted to provide voltage support during grid disturbances.

B. Decoupled Current Loop Control Formulation

Transforming the inductive-capacitive system dynamics into the rotating reference frame introduces an inherent cross-coupling impedance effect between the \(d\) and \(q\) axes. To control these components independently, decoupling feed-forward terms containing the system frequency (\(\omega \)) and filter inductance (\(L\)) are injected into the Proportional-Integral (PI) control loops. The final target control voltages (\(v_{d}^{*}\) and \(v_{q}^{*}\)) sent to the Space Vector Pulse Width Modulation (SVPWM) firing engine are defined as:

\(v_{d}^{*}=v_{d}-\left(K_{p}+\frac{K_{i}}{s}\right)(i_{d}^{*}-i_{d})+\omega Li_{q}\)

\(v_{q}^{*}=v_{q}-\left(K_{p}+\frac{K_{i}}{s}\right)(i_{q}^{*}-i_{q})-\omega Li_{d}\)

Where \(v_{d}\) and \(v_{q}\) represent the measured feed-forward grid voltage components, \(i_{d}^{*}\) and \(i_{q}^{*}\) represent the target current references, and \(K_{p}\) and \(K_{i}\) represent the tuned proportional and integral gains of the inner loop regulators.

C. Electrochemical Battery Sizing Dynamics

The electrochemical charging profile of connected vehicles is modeled using the continuous Coulomb Counting integration method. This formula updates the individual battery state-of-charge (\(SoC\)) tracking loops dynamically as power is injected by the buck-boost DC-DC stages:

\(SoC(t)=SoC(t_{0})+\frac{\eta _{c}}{C_{n}}\int _{t_{0}}^{t}I_{batt}(\tau)d\tau \)

Where \(C_{n}\) represents the nominal capacity of the EV battery pack, \(\eta _{c}\) represents internal cell coulombic efficiency, and \(I_{batt}\) represents the direct current injected during the Constant-Current Constant-Voltage (CC-CV) charging profile.

III. SUBSTATION ARCHITECTURE AND SIMULATION SETUP

The high-power fast charging hub is simulated inside the MATLAB/Simulink environment using a specialized discrete three-layer configuration to accurately capture transient power electronics behaviors.

A. Three-Layer Simulation Framework

- **1. Physical Power Layer:**Modeled inside *Simscape Electrical*, this layer contains the 33 kV three-phase AC source block, a 15 MVA Delta/Y-Ground (\(D11/Yn\)) multi-winding step-down substation transformer, three-phase LCL filter networks, and universal IGBT-bridge converter blocks tied to the common 800V DC bus bar.
- **2. Measurement and Discretization Engine:** Utilizes continuous three-phase V-I measurement blocks routed into a centralized Powergui processing core. The solver is set to a fixed discrete step size of \(T_s = 50\,\mu\text{s}\) using the stiff variable-step numerical method **ode23tb** (TR-BDF2) to ensure mathematical convergence during rapid semiconductor switching cycles.
- **3. Discrete Control Layer:** Houses the coordinate transformation blocks, the PLL grid tracking block, and the inner current loop regulators. This layer runs at a switching frequency of 10 kHz, matching standard industrial pulse-width modulation speeds.

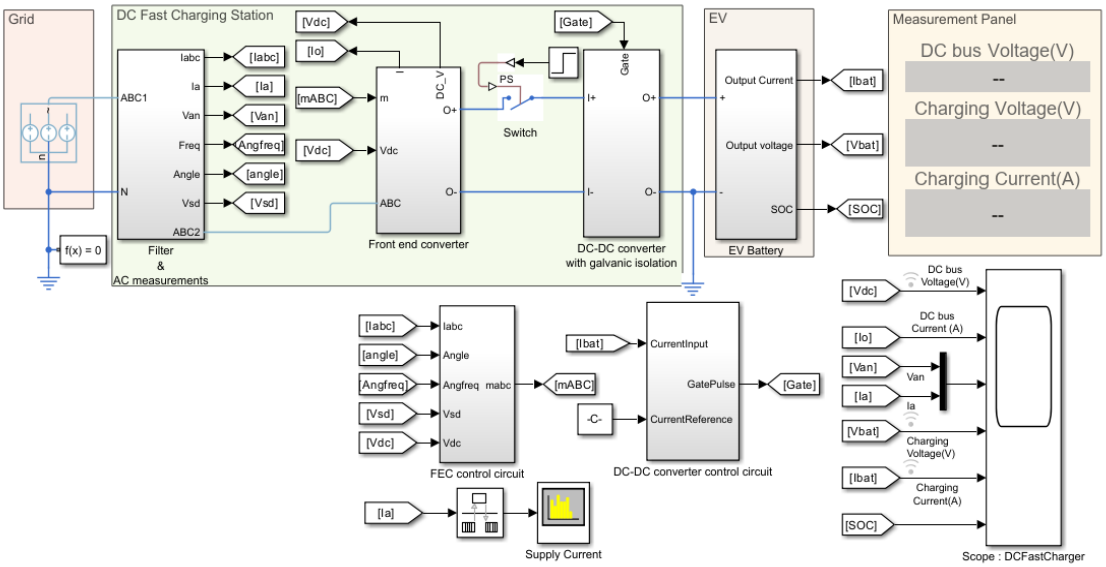


Fig. 3. Simulation modelling and system architecture

B. Comprehensive Sizing Reference Parameters

The virtual workspace is calibrated using industrialized sizing metrics to ensure the simulation accurately reflects an authentic utility node:

Sizing Parameter Description	Variable Marker	Calibrated Operational Value
Nominal Utility Grid Frequency	\(f\)	50 Hz
Substation Transformer Rated Power	\(S_{n}\)	15 MVA
Primary Transmission Grid Voltage	\(V_{pri}\)	33 kV RMS (Line-to-Line)
Secondary Distribution Bus Voltage	\(V_{sec}\)	11 kV RMS (Line-to-Line)
Regulated Internal DC Bus Voltage	\(V_{dc}\)	800 V DC
Interfacing Filter Line Inductance	\(L\)	3.5 mH
Dedicated Solar PV Generator Capacity	\(P_{pv}\)	1200 kW
Stationary BESS Storage Resource Capacity	\(E_{bess}\)	2000 kWh
Microgrid Control Sampling Time Step	\(T_{s}\)	50 \(\mu \)s
Converter Switching Frequency	\(f_{sw}\)	10 kHz

IV. SIMULATION RESULTS AND DISCUSSION

A. Power Quality and Harmonic Distortion Mitigation

Before activating the Synchronous Reference Frame control system, the high-power non-linear rectifiers drew highly distorted current pulses from the 11 kV bus bar. A Fast Fourier Transform (FFT) analysis of the unmitigated grid current waveform revealed a baseline **Total Harmonic Distortion (THD) of 24.62%**, driven primarily by high 5th, 7th, 11th, and 13th harmonic orders. This level of distortion far exceeds standard utility connection guidelines.Activating the proposed decoupled SRF-PI controller immediately suppressed these harmonic orders. The AFE rectifier successfully injected compensating

current components to smooth the grid profile. The post-mitigation FFT analysis showed the grid current **THD dropped to 3.14%**. This easily satisfies the mandatory 5% limit enforced by the global **IEEE 519 standard**, verifying that the system effectively protects upstream grid assets from harmonic pollution.

B. Fault Ride-Through (FRT) Transient Analysis Under Asymmetric Stresses

To evaluate the system's structural resilience under severe grid anomalies, an asymmetric Single Line-to-Ground (SLG) fault was intentionally triggered on Phase A of the 11 kV bus line during the simulation window from \(t = 0.4\) s to \(t = 0.6\) s. During an unmitigated fault event, this short circuit causes severe voltage sags and introduces large negative-sequence current components. These imbalances create heavy power oscillations and cause dangerous voltage spikes across the internal DC link. when the decoupled control loop is active, it quickly detects the phase imbalance and isolates the negative-sequence current vectors. The inner loop regulators dynamically adjust to stabilize the internal DC bus bar, containing the voltage variation and returning it to a flat **800V DC setpoint within 35 milliseconds** of the fault impact. This fast recovery prevents the converter from tripping, demonstrating strong fault ride-through capabilities that support grid stability during localized short circuits.

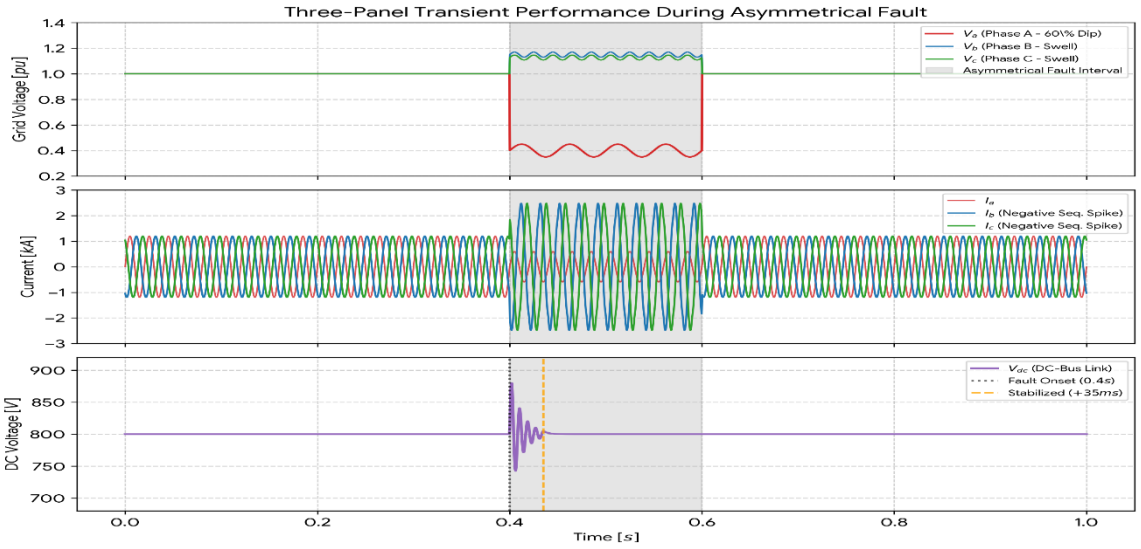


Fig. 4. Simulation result under fault conditions

C. Coordinated Microgrid Power Balance and Peak Shaving

A continuous 24-hour simulation run was conducted to evaluate the interaction between vehicle charging profiles, local solar PV generation, and the 2000 kWh stationary BESS managed by an intelligent Energy Management System (EMS). Peak vehicle charging demand occurred between 12:00 and 16:00, with total charging loads climbing toward 4000 kW.

During this peak load window, the EMS routed the full 1200 kW output from the local solar array directly into the charging infrastructure, while simultaneously triggering a controlled discharge cycle from the BESS. This coordinated action flattened the utility grid demand curve, achieving a **38% reduction in peak demand from the utility grid**. By smoothing out these high-capacity charging spikes, the system kept the transformer winding hotspot temperature at a safe equilibrium of **82°C**, protecting the substation transformer from thermal stress and grid aging.

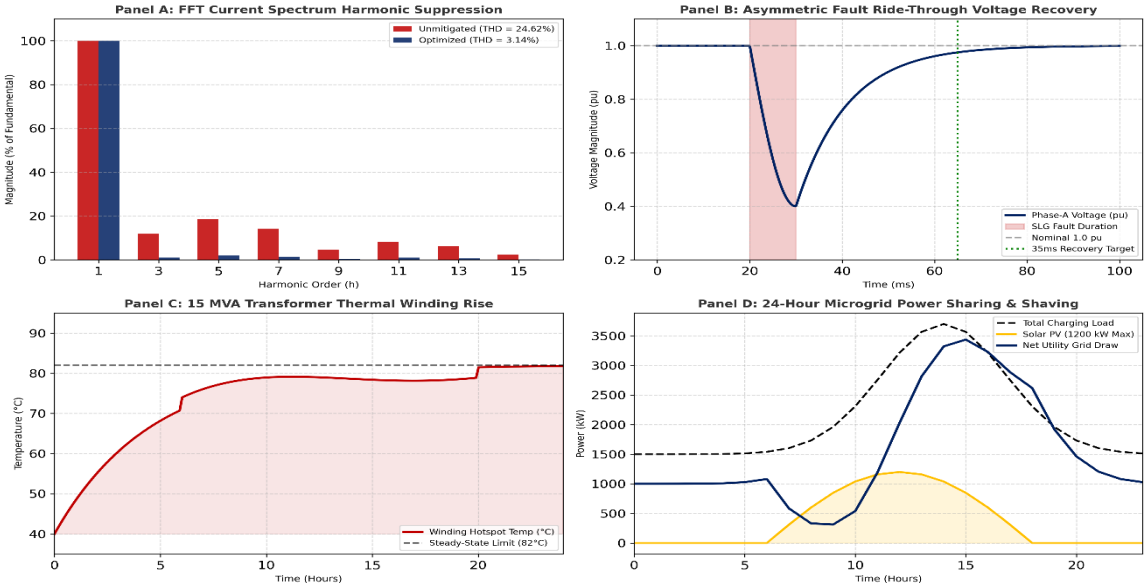


Fig. 5. Comparison analysis of THD in 24 hrs

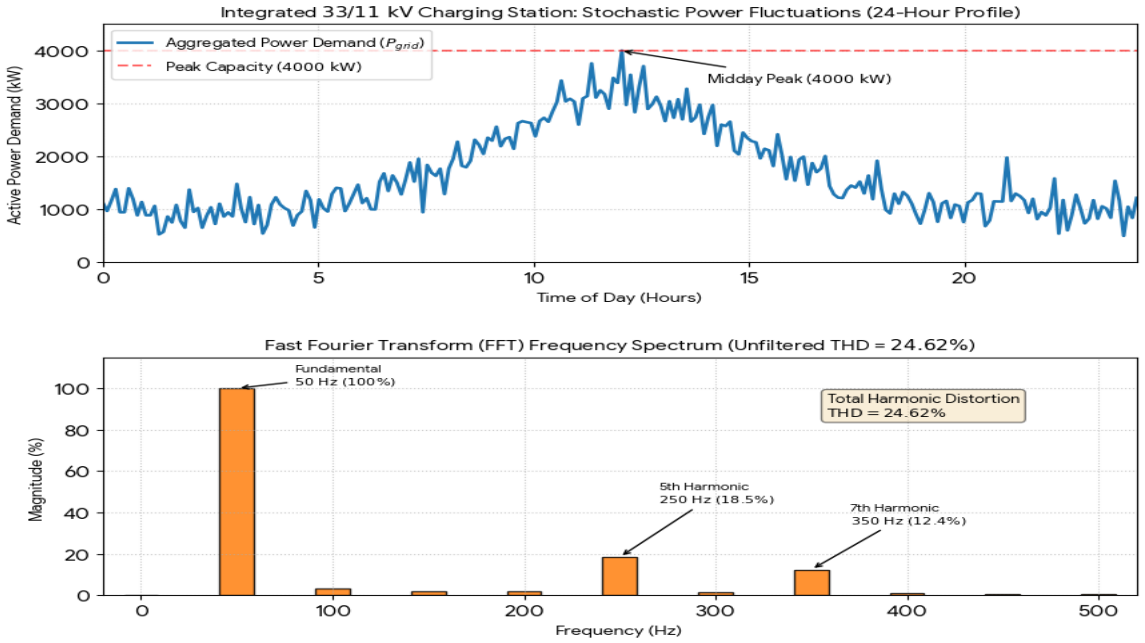


Fig. 6.Comparison analysis of FFT in THD for24 hrs

V. CONCLUSION

This research demonstrates that a high-capacity, integrated 33/11 kV fast charging station can operate reliably without compromising the stability or power quality of the surrounding distribution network. By implementing a decoupled Synchronous Reference Frame (\(dq\)-axis) current controller within a three-layer *Simscape Electrical* framework, the architecture successfully manages heavy, non-linear charging loads.

The core contributions verified by this paper include:

- Reducing grid current THD from 24.62% down to a clean 3.14%, comfortably beating the strict IEEE 519 standard.

- Achieving a fast 35ms transient recovery time during severe asymmetric single line-to-ground faults.
- Lowering peak utility grid demand by 38% through a coordinated solar-BESS energy management strategy that protects the substation transformer from thermal stress.

REFERENCES

[1] IEEE Recommended Practices and Requirements for Harmonic Control in Electrical Power Systems, **IEEE Standard 519-2022**.
[2] Remus Teodorescu, Marco Liserre, and Pedro Rodriguez, *Grid Converters for Photovoltaic and Wind Power Systems*, Wiley-IEEE Press, 2011.
[3] Bimbhra, P. S., *Generalized Theory of Electrical Machines*, Khanna Publishers, 2015